NANO LETTERS

2008
Vol. 8, No. 2
656−660

Electron–Phonon Coupling and Localization of Excitons in Single Silicon Nanocrystals

Jörg Martin,[†,‡] Frank Cichos,[†,§] Friedrich Huisken,[∥,⊥] and Christian von Borczyskowski*,[†]

Institute of Physics and nanoMA, Chemnitz University of Technology, D-09107 Chemnitz, Germany, Fraunhofer Institute IZM, D-09126 Chemnitz, Germany, Institute of Experimental Physics I, Leipzig University, D-04103 Leipzig, Germany, Max Planck Institute for Astronomy, D-69117 Heidelberg, Germany, and Institute of Solid State Physics, University of Jena, D-07743 Jena, Germany

Received November 29, 2007; Revised Manuscript Received December 21, 2007

ABSTRACT

We report a detailed photoluminescence (PL) study on single silicon nanocrystals produced by laser pyrolysis. The PL spectra reveal nearly homogeneously broadened zero-phonon lines coupled to Si–O–Si phonon transitions in the SiO_2 shell. A systematic investigation of electron–phonon coupling is reported on the basis of single nanocrystals. The stepwise localization of electron and hole at the Si–SiO_2 interface for nanocrystals smaller than $d \approx 2.7$ nm is driven by electron–phonon coupling. From the localization energies the effective Bohr radii of the (localized) electron and hole are estimated to be in the range of 1–2 bond lengths of Si–O and Si–Si.

During the past two decades, the photoluminescence (PL) of silicon (Si) nanocrystals (nc's) has been discussed intensively.[1,2] One of the outstanding but not yet solved questions is whether the excitonic PL is completely related to quantum confinement (QC) of, e.g., the Si nc or whether other mechanisms (e.g., surface-related energy potentials or states) are also involved. According to our interpretation of QC, the conduction band edge continually increases in energy when the size of the Si nc is reduced while the opposite behavior applies to the valence band edge. The concerted action of both effects results in an increase of the band gap energy with decreasing size. The PL in a quantum-confined system, i.e., the radiative recombination of the electron and hole, reflects this situation and increases in energy with decreasing size.

Surface-related states, on the other hand, may have energies above or below the band edges of the conduction and valence bands of bulk Si, respectively. Usually they will not influence the PL spectrum. However, if the particle size decreases and the band gap increases, they may affect the QC to appear as inner band gap states and then drastically change the PL behavior. This situation can be understood as a kind of "breakdown of QC" since the PL energy as a function of decreasing particle size does no longer increase, which does not imply that the QC of Si itself breaks down. Such a behavior, which we will in this paper consider as a "breakdown of QC," will limit the PL tunability and thus applications in Si optical nanostructures especially in the short wavelength range. Unfortunately, the mechanisms which generally drive a crossover from delocalized to localized states are not sufficiently well understood. Fundamental knowledge of these effects will have an impact on both basic and material science with respect also to many other quantum-confined systems.

PL properties of Si nc's depend critically on preparation techniques.[3−6] However, all systems have in common that PL is only observed when the nc's are passivated, e.g., by SiO_2[6] or hydrogen.[7] In the case of porous Si nc's, it has been argued that the presence of oxygen impurities in the SiO_2 shell results in a breakdown of QC for small nc's.[7] Since ensemble data provide only limited information, evidence for a localization of the exciton stems from comparison with theoretical calculations.[7,8] However, it is still an open question whether this observation holds for Si nc's in general. Moreover, and even more important, is the identification of the restricting mechanisms upon QC. To unravel these still open fundamental questions, experiments on uniquely prepared Si nc's in combination with a most elaborate optical technique will be mandatory.

* Corresponding author. Phone: +49 371-531-33035. Fax: +49-371-531-21819. E-mail: borczyskowski@physik.tu-chemnitz.de.
[†] Chemnitz University of Technology.
[‡] Fraunhofer Institute IZM.
[§] Leipzig University.
[∥] Max Planck Institute for Astronomy.
[⊥] University of Jena.

10.1021/nl0731163 CCC: $40.75
Published on Web 01/16/2008

Conventional optical techniques provide very often only limited information since experiments are performed on nc ensembles with a remaining size distribution hampering spectral resolution. For Si nc ensembles, the PL is very broad due to the remaining size dispersion (typically 1.4−2.5 eV),[1−4,6−9] and therefore detailed spectroscopic access can only be gained by optical single particle detection schemes[9] as applied within this study.

Most uniquely defined Si nc's have been prepared by CO_2 laser pyrolysis of silane in a gas flow reactor.[6] For nc diameters larger than 3 nm[6] it has been confirmed that the PL in these systems is related to QC. Additionally, it is generally assumed that the energy−size relation also holds below 3 nm, though clear experimental proof is lacking. The central topic of the present study is to follow the PL of small (d < 3 nm) single Si nc's using optical single particle detection in order to unravel the limiting conditions for QC.

With respect to Si nc's, single particle techniques have been applied to nanocrystals prepared by various methods such as wafer etching (por-Si nc),[9−11] lithography (lit-Si nc),[5] or by colloidal chemistry (col-Si nc).[12] This letter will focus on the spectroscopy of single Si nc's prepared by laser pyrolysis (pyr-Si nc).[6]

Details of the synthesis are given elsewhere.[6,13] Pyr-Si nc's have a crystalline core surrounded by a natural layer of amorphous SiO_2.[13] Ensemble PL spectra typically reveal a broad PL spectrum with a maximum around 1.5 eV. This corresponds to an average nc diameter of 5.7 nm. The PL decay rate increases exponentially with increasing PL energy.[14] For single particle PL spectroscopy pyr-Si nc's have been dispersed in toluene followed by mixing with a PMMA−toluene solution. This mixture was then spin-cast onto a quartz slide to obtain about a 20 nm thick polymer film. The home-built confocal microscope has been described in detail elsewhere.[9] The fluorescence of pyr-Si nc's was excited at 482 nm (2.572 eV) with a krypton ion laser. The fluorescence was imaged onto a grating monochromator (Acton SP-300i) with a liquid-nitrogen-cooled CCD detection system (Princeton Instruments). Separation of the fluorescence from the excitation light was achieved by a dichroic beam splitter and a long-pass filter with a cutoff wavelength at 505 nm (2.455 eV).

Figure 1 shows representative PL spectra of two individual pyr-Si nc's. The identification as a single particle is based on the observation of PL intermittency (see insert of Figure 1) which can only be observed for single quantum objects. In agreement with recent experiments,[9−11] the PL spectra of single Si nc's have at room temperature a zero phonon line width of about 100 meV and show on the low-energy side satellite bands with energy separations between 130 (spectrum (1)) and 160 meV (spectrum (2)). The range of separations can be clearly related to LO or TO Si−O−Si phonon modes of SiO_2.[15]

The homogeneously broadened line width of lit-Si nc's is found to be about 100 meV at room temperature according to Sychugov et al.[16] The narrowest zero-phonon line observed for pyr-Si is therefore very close to the homogeneously broadened line width. Except the experiments on lit-Si nc's,[5,16] all other single Si nc studies showed either lines much broader than 100 meV or Si−O−Si vibrational transitions between 130 and 160 meV.[10−12] Further, these studies on single Si nc's reported only PL energies above 1.8 eV as in the present case. In most cases, the corresponding ensemble emission extended over a very broad range. This, however, does not necessarily mean that single nc's cannot be detected below 1.8 eV. Instead the related PL might become considerably weaker with decreasing energy. A general explanation for this observation is based on the following arguments. Several authors[14,17,18] have shown that the PL decay rate k increases up to 1.8 eV exponentially with the PL energy according to $k \approx \exp(E/E^*)$ with $E^* \approx$ 250 meV. Above 1.9 eV the decay rate increases even faster with PL energy.[14] It thus appears that for large Si nc's with longer lifetimes and an increased absorption cross section several excitons in the same nc might be created at constant excitation intensity.[9] This will result in nonradiative Auger processes, preventing the efficient detection of large single Si nc's.

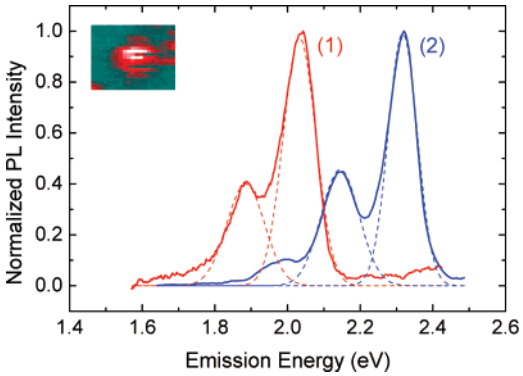

Figure 1. PL spectra of two single pyr-Si nc's. The broken lines show Gaussian fits to the experimental data. The insert shows the confocal scan over a single Si nc exhibiting PL intermittency as indicated by dark and bright stripes.

While the satellite lines close to 130 meV resemble those of the Si−O−Si TO phonon also observed in bulk SiO_2 material,[15] phonons close to 160 meV correspond to the LO transition.[15] Since phonons are detected via the PL transition of Si nc's, they must be strongly coupled to the electronic transition via electron−phonon interaction and should have LO character. The phonon frequencies for 55 individual pyr-Si nc's vary as shown in Figure 2 linearly from 130 to 170 meV upon increase of the PL energy from 1.95 to 2.4 eV.

We attribute this variation to the existence of surface phonons ω_s which have been predicted to be a mixture of LO and TO modes.[19] Klein et al.[19] provided a model to calculate surface phonon frequencies ω_s as a function of the dielectric properties in a two-component system via

$$\omega_s = \left(\frac{\epsilon_\infty \omega_{LO}^2 + 2\epsilon_M \omega_{TO}^2}{\epsilon_\infty + 2\epsilon_M} \right)^{1/2} \quad (1)$$

where ω_{LO} and ω_{TO} are the bulk phonon frequencies in SiO_2, ϵ_∞ is the high-frequency dielectric constant of SiO_2, and ϵ_M is the dielectric constant of the embedding medium which,

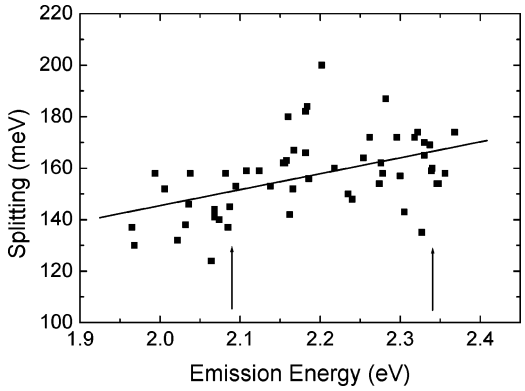

Figure 2. SiO_2 splitting between the first phonon and the zero phonon PL band as function of PL energy of Si nc's. Arrows mark the PL intensity maxima described in Figure 3. Note that the fluctuations of the vibronic splittings at a constant PL energy are considerably larger than the experimental error (see also discussion related to the Huang−Rhys factor).

in our case, is Si. Taking $\epsilon_\infty = 2.13$ and $\epsilon_M = 9.6$ (as determined for a 4.5 nm Si nc),[19] ω_S becomes 138 meV instead of the expected $\omega_{LO} \approx 160$ meV. Decreasing the size of the Si nc will decrease the Si/SiO_2 ratio and thus the influence of Si. This is observed in our study where, for small Si nc's, ω_S approaches $\omega_{LO} \approx 160$ meV.

For some of the Si nc's (see Figure 1 and refs 10−12) a clear phonon progression could be detected. The intensities of the Si−O−Si phonon bands relative to the zero-phonon line are a direct measure of the strength of the electron−phonon coupling. Phonon side bands involving n phonons $\hbar\omega_s$ have intensities $I_n = S_n \exp(-S)/n!$, where S corresponds to the Huang−Rhys factor.[20]

Electron−phonon (Fröhlich-type) coupling is due to a phonon-induced deformation of the crystal lattice acting on the charge distribution of the exciton and results in a lowering of the excitonic energy. Since obviously Si−O−Si phonons at the Si− SiO_2 interface couple to the PL emission, the following questions arise: (i) Is the PL itself due to (surface-related) localized states or to purely quantum-confined states, and (ii) does the electron−phonon coupling strength depend on the size of the Si nc?

We have investigated the PL spectra of 93 individual Si nc's between 1.95 and 2.4 eV. A histogram (abundance) of the corresponding PL zero phonon line energies is displayed in Figure 3 (top). Such a diagram is obtained by counting the number of PL spectra of single Si nc's at a certain PL energy. This type of data analysis which is commonly applied in single quantum object detection provides the distribution of emitters without taking absolute PL intensities into account. The peaks in this distribution at about 2.125 and 2.325 eV immediately imply that more nc's emit at these PL energies than at other ones. Additionally, a striking similarity to the nc histogram is observed with very similar peak positions when summing up all the PL zero-phonon line intensities, Figure 3 (top).

It is well-known that the preparation of pyr-Si nc result in a log-normal size distribution.[26] For the material used in our experiments this distribution is centered at $d = 5.1$ nm

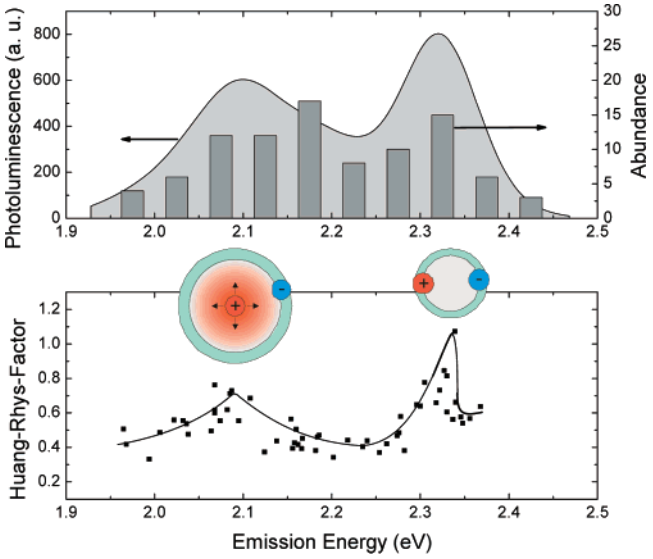

Figure 3. Abundance (columns) of detected single Si nc's and the related PL spectrum obtained from a sum of the zero-phonon lines (top). Dependence of the Huang−Rhys factor S on PL energy (bottom). The line serves only as a guideline. A scheme of the localization model is included.

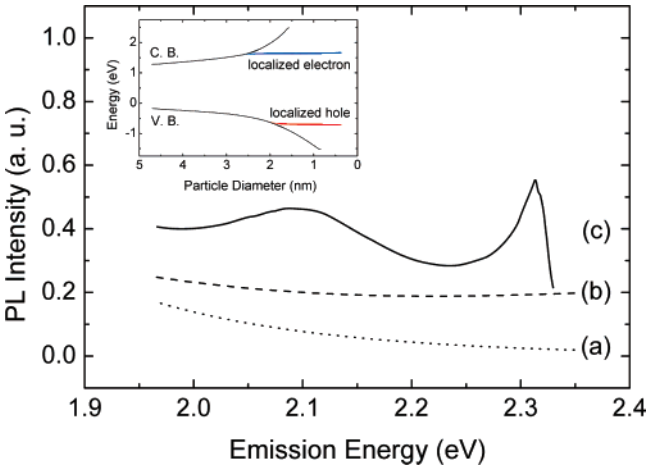

Figure 4. Dotted line (a): Calculated PL intensity for a nonsymmetric log-normal size distribution[26] centered at $d = 5.1$ nm (width 4.4 nm). Dashed line (b): PL intensity weighted with the decay rate dependence (see text). Solid line (c): PL intensity (b) assuming additionally size dependent electron and hole localization at 2.1 and 2.325 eV, respectively. The insert shows the tentative behavior of conduction and valence band energies upon localization.

and has a width of 4.4 nm. Assuming that QC according to ref 21 is still valid, we have plotted in Figure 4 the expected PL intensity ((a); dotted line) according to the known size distribution. Additionally, we take the single particle detection sensitivity into account, arguing that the PL intensities increase exponentially in accordance with the increasing PL decay rates (see previous discussion). The modified PL intensity ((b); dashed line in Figure 4) is obtained by weighting the originally expected PL spectrum (a) with the detection sensitivity which increases with PL energy.

How can the nonmonotoneous distribution of PL energies observed in Figure 3 be explained? Garrido et al.[8] report that the band gap absorption still follows predictions from

QC for Si nc's with $d < 3$ nm. The experimentally observed PL, however, is well below the theoretically expected energies. A similar behavior has been found by Ledoux et al.[6] Together with results of Wolkin et al.[7] these observations indicate a possible breakdown of QC, which results in size independent PL energies as a function of further decreasing the nc diameter. To mimic this behavior, we take into account that the PL (Figure 3) reveals two distinct maxima. Let us now assume that the low-energy peak at 2.1 eV corresponds to electron localization (see insert in Figure 3). Above this energy the corresponding conduction band energy level will become constant despite still lowering the nc diameter (see insert in Figure 4). The same applies for the valence band (hole) at the respective high-energy peak at 2.325 eV. Imposing these restrictions to the calculated PL intensities ((b) in Figure 4) results in the PL intensity distribution (c) with a clear double peak structure (solid line in Figure 4) essentially resembling the measured distribution of energies as shown in Figure 3 (top). Though this is only indirect proof, we claim that the experimentally observed double peak structure in PL arises from a separate localization of electron and hole. Obviously it would be desirable to determine the size of Si nc's by SEM for each individual nc on which PL spectra are reported which is, unfortunately, not feasible. However, the general relationship between size and PL energy has experimentally been determined for Si nc's.[6,7]

Let us now discuss the influence of the nc diameter (PL energy) on the electron−phonon coupling. We determined the corresponding coupling parameter S for 55 nc's at PL energies between 1.95 and 2.4 eV. The other 38 Si nc's showed also a strong electron−phonon coupling to Si−O−Si phonons. However, a precise determination of S was hampered by distorted spectral line shapes probably caused by a competition between coupling to both Si−O−Si (130−160 meV) and Si (∼50 meV) phonons. The occasional appearance of Si-phonons has also been reported recently.[16] Figure 3 (bottom) collects the Huang−Rhys factors determined from $S = I_1/I_0$ as a function of PL energy. S peaks at PL energies close to 2.08 and 2.33 eV very similar to the peak positions of the PL. The large fluctuations at a given PL energy are beyond the experimental uncertainty and reflect (i) variations of S from nc to nc and (ii) additional time-dependent spectral fluctuations of the PL, as has been clearly observed in some cases. Variations of S easily arise upon variation of the SiO_2 shell structure which is certainly not homogeneous. Additionally, from PL investigations on various types of nc including Si, such crystals can be charged without changing the PL energy considerably.[9] Occasionally these effects show up as a fluctuation of the PL energy and intensity in time. A charged nc will have a different electron−phonon coupling.

The striking similarity between S and the PL as a function of energy (nc diameter) occurs since electron−phonon coupling, naturally involved in any kind of self-trapping process, obviously also drives the breakdown of QC. In general, electron−phonon coupling of excitons in semiconductors relies on the (Fröhlich) coupling of an electric field generated by a nonuniform charge density distribution of electron and hole with a fluctuating electric field induced by the lattice phonons. In semiconductor nc's the electric field generated by the delocalized electron and hole usually decreases with increasing size.[22] The situation completely changes, when, as in the present case for Si nc's, the electron and hole become sequentially localized (in the SiO_2 shell or at the (SiO_2−Si; SiO_2/PMMA) interface). In a simple picture, the average distance R between electron and hole will be suddenly increased to $R \approx d/2$ upon localization of the electron at 2.1 eV. Related to this S will also increase. The distance R (and S) will be further reduced with decreasing size. Upon localization of the hole at 2.325 eV, the average electron−hole distance R (and thus S) will be increased again and will result in $R > d/2$, assuming that electron and hole localization are spatially not correlated. When the size is still further decreased, R and S will become smaller again. This overall behavior is schematically shown in the insert of Figure 3.

The present experiments have been carried out with samples where the Si nc's were embedded in a PMMA matrix. It will be interesting to study the influence of the dielectric environment on the PL behavior by employing different polymer films. Such studies are planned for the near future. The effect of the environment will surely be mediated by the SiO_2 shell and will thus depend on the thickness of this shell. For larger pyr-Si nc's, we have shown by high-resolution electron microscopy that the thickness of the oxide shell is approximately 10% of the total diameter.[13] Unfortunately, we do not know whether this rule of thumb, which would yield a SiO_2 thickness of less than 0.5 nm, can be applied to the small Si nc's investigated in the present study. However, the influence of the relative ratio of the amount of Si to SiO_2 can be already seen from the dependence of ω_S upon the Si nc size (see Figure 2 and eq 1). This is also a strong indication of the increasing influence of the SiO_2 shell with shrinking size of the Si nc's and may be considered as a modification of the overall confining potential.

While the onset of localization has been estimated from ensemble PL spectra to take place at about 1.8−1.9 eV,[6−8] being complete at 2.2 eV,[7] the present results on single pyr-Si nc's are in a similar range but show localization energies at about 2.1 and 2.325 eV, respectively. From our study we cannot decide whether the electron or hole becomes localized at first. Since the electron has the smaller effective mass and a spatially more extended wave function, it might thus "feel" the interface more readily and should become localized first.

It is reasonable to assume that localization will take place when the respective radii a_e and a_h of electron and hole are comparable to the diameter d of the Si nc's. One might even estimate the radii of the localized charges from the two localization energies at 2.1 and 2.325 eV. Delerue et al.[21] have presented a semiempirical EMA model to describe QC in nc's. This model turned out to be reliable for a large range of sizes when comparing experiments and theoretical predictions though care has to be taken at very small sizes. Nevertheless, since we like to make only a qualitative estimate of the radii of the wavefunction of the charges after localization, these analytical EMA confinement models are

more appropriate. According to these models[23] the quantum confinement energy E_{QC} is

$$E_{QC} = \frac{\hbar^2\pi^2}{2d^2}\left(\frac{1}{m_{h^*}} + \frac{1}{m_{e^*}}\right) - \frac{1.786e^2}{4\pi\epsilon_o\epsilon}\frac{1}{d} \qquad (2)$$

For the localization of the electron and hole we assume that $d \approx a_e$ and $d \approx a_h$, respectively. For these radii we identify the energy at which localization takes place with the confinement energy $E_{QC_e} = (2.1-1.12)$ eV and $E_{QC_h} = (2.325-1.12)$ eV for the electron and hole, respectively. The energy 1.12 eV corresponds to the band gap of bulk Si. Making use of these two localization energies, we determine $a_e = 0.26$ nm and $a_h = 0.20$ nm with ϵ (Si) = 11.7. For $\epsilon = 3.75$ (which refers to SiO_2) we obtain $a_e = 0.51$ nm and $a_h = 0.45$ nm, respectively. For these estimates, we have taken parameters reported for Si clusters[24] with $m_{e^*} = 0.19m_o$ and $m_{h^*} = 0.286m_o$ (m_o being the rest mass of the electron). We have also assumed that the contribution of the electron energy following electron localization remains constant.

The estimated localization radii are in the same range as the bond lengths of Si−O and Si−Si bonds of 0.163 and 0.233 nm, respectively. This implies that localization (of electron or hole) is on nearly 1−2 bond lengths, but not necessarily on the same bond. These values are by a factor of 2−3 smaller than the range of electron−hole separation $R \approx 0.6-0.9$ nm that were obtained earlier from magnetic resonance experiments on probably localized Si triplet states.[11] Our results for Si nc's can be compared with the hole localization in CdSe nc's reported by Nirmal et al.,[25] where, upon localization, a reduction of a_h from 0.6 to 0.33 nm has been observed at temperatures below 35 K. In that case the localization also takes place at the corresponding interface.

In conclusion, we have shown, that the emission spectra of Si nc's with a SiO_2 shell reveal a strong electron−phonon coupling to Si−O−Si phonons. An analysis of electron−phonon coupling has been performed on the basis of single quantum emitters. The strong coupling drives the successive localization of the electron and hole upon decreasing the diameter of the Si nc's. This localization implies that quantum confinement breaks down — in the sense we have described it in the introduction — depending on the strength of electron−phonon coupling. Referring to the results of Wolkin et al.,[7] we assume that a less polar passivation than SiO_2 will possibly prevent electron and hole localization and extend tunability of Si nc emission toward shorter wavelengths, which is of great importance to optoelectronic applications. We also like to emphasize that our results could only be obtained by applying optical single particle detection. Though the presented model might be considered to be very crude, it can be regarded as a first step for further study of the interplay among quantum confinement, carrier localization, and electron−phonon coupling in quantum dots.

Acknowledgment. The authors gratefully acknowledge financial support by the Deutsche Forschungsgemeinschaft (DFG) within the Research Group "Laboratory Astrophysics".

References

(1) Lockwood, D. J., Ed. *Light Emission in Silicon: From Physics to Devices*; Academic Press: New York, 1998.
(2) Heitmann, J.; Müller, F.; Zacharias, L.; Yi, M.; Kovalev, D.; Eichhorn, F. *Phys. Rev. B* **2004**, *69*, 195309.
(3) Canham, L. T. *Appl. Phys. Lett.* **1990**, *57*, 1046.
(4) Cheylan, S.; Elliman, R.; Gaff, K.; Durandet, A. *Appl. Phys. Lett.* **2001**, *78*, 1670.
(5) Valenta, J.; Juhasz, R.; Linnros, J. *Appl. Phys. Lett.* **2002**, *80*, 1070.
(6) Ledoux, G.; Gong, J.; Huisken, F.; Guillois, O.; Reynaud, C. *Appl. Phys. Lett.* **2002**, *80*, 4834.
(7) Wolkin, M. V.; Jorne, J.; Fauchet, P. M.; Allan, G.; Delerue, C. *Phys. Rev. Lett.* **1999**, *82*, 197.
(8) Garrido, B.; López, M.; Pérez-Rodrígez, A.; García, C.; Pellegrino, P., et al. *Nucl. Instrum. Methods Phys. Res., Sect. B* **2004**, *216*, 213.
(9) Cichos, F.; Martin, J.; von Borczyskowski, C. *Phys. Rev. B* **2004**, *70*, 115314. Martin, J.; Cichos, F.; von Borczyskowski, C. *J. Luminesc.* **2004**, *108*, 347.
(10) Mason, M. D.; Credo, G. M.; Weston, K. D.; Buratto, S. K. *Phys. Rev. Lett.* **1998**, *80*, 5405.
(11) Martin, J.; Cichos, F.; Chan, I. Y.; Huisken, F.; von Borczyskowski, C. *Isr. J. Chem.* **2004**, *44*, 341.
(12) English, D. S.; Pell, L. E.; Yu, Z.; Barbara, P. F.; Korgel, B. A. *Nano Lett.* **2002**, *2*, 681.
(13) Hofmeister, H.; Huisken, F.; Kohn, B. *Eur. Phys. J. D* **1999**, *9*, 137.
(14) Huisken, F.; Ledoux, G.; Guillois, O.; Reynaud, C. *Adv. Mater.* **2002**, *14*, 1861.
(15) Kirk, C. T. *Phys. Rev. B* **1988**, *38*, 1255.
(16) Sychugov, I.; Juhasz, R.; Valenta, J.; Linnros, J. *Phys. Rev. Lett.* **2005**, *94*, 087405.
(17) Sa'ar, A.; Reichman, Y.; Dovrat, M.; Krapf, D.; Jedrzejewski, J.; Balberg, I. *Nano Lett.* **2005**, *5*, 2443.
(18) Vial, J. C.; Bsiesy, A.; Gaspard, F.; Hérino, R.; Ligeon, M., et al. *Phys. Rev. B* **1992**, *45*, 14171.
(19) Klein, M. C.; Hache, F.; Ricard, D.; Flytzanis, C. *Phys. Rev. B* **1990**, *42*, 11123.
(20) de Maat-Gersdorf, I.; Gregorkiewicz, T.; Ammerlaan, C. A. J.; Sobolev, N. A. *Semicond. Sci. Technol.* **1995**, *10*, 666.
(21) Delerue, C.; Allan, G.; Lanoo, M. *Phys. Rev. B* **1993**, *48*, 11024.
(22) Woggon, U.; Lüthgens, E.; Wenisch, H.; Hommel, D. *Phys. Rev. B* **2001**, *63*, 073205.
(23) Trwoga, P. F.; Kenyon, A. J.; Pitt, C. W. J. *Appl. Phys.* **1998**, 83, 3789.
(24) Xia, J. B. *Phys. Rev. B* **1989**, *40*, 8500.
(25) Nirmal, M.; Murray, C. B.; Bawendi, M. G. *Phys. Rev. B* **1994**, *50*, 2293.
(26) Ledoux, G.; Guillois, O.; Porterat, D.; Reynaud, C.; Huisken, F.; Kohn, B.; Paillard, V. *Phys. Rev. B* **2000**, *62*, 15942.

NL0731163